Valence-band ordering and magneto-optic exciton fine structure in ZnO

Walter R.L. Lambrecht,[1] Anna V. Rodina,[2,*] Sukit Limpijumnong,[1,3] B. Segall,[1] and Bruno K. Meyer[2]
[1]*Department of Physics, Case Western Reserve University, Cleveland, Ohio 44106-7079*
[2]*I. Phys. Institute, Justus Liebig University of Giessen, 35392 Giessen, Germany*
[3]*School of Physics, Institute of Science, Suranaree University of Technology, Nakhon Ratchasima, Thailand*
(Received 23 August 2001; published 23 January 2002)

Using first-principles linear muffin-tin orbital density functional band structure calculations, the ordering of the states in the wurtzite ZnO valence-band maximum, split by crystal-field and spin-orbit coupling effects, is found to be $\Gamma_{7(5)}>\Gamma_{9(5)}>\Gamma_{7(1)}$, in which the number in parentheses indicates the parent state without spin-orbit coupling. This results from the negative spin-orbit splitting, which in turn is due to the participation of the Zn $3d$ band. The result is found to be robust even when effects beyond the local density approximation on the Zn $3d$ band position are included. Using a Kohn-Luttinger model parametrized by our first-principles calculations, it is furthermore shown that the binding energies of the excitons primarily derived from each valence band differ by less than the valence-band splittings even when interband coupling effects are included. The binding energies of $n=2$ and $n=1$ excitons, however, are not in a simple 1/4 ratio. Our results are shown to be in good agreement with the recent magneto-optical experimental data by Reynolds *et al.* [Phys. Rev. B **60**, 2340 (1999)], in spite of the fact that on the basis of these data these authors claimed that the valence-band maximum would have Γ_9 symmetry. The differences between our and Reynolds' analysis of the data are discussed and arise from the sign of the Landé g factor for holes, which is here found to be negative for the upper Γ_7 band.

DOI: 10.1103/PhysRevB.65.075207 PACS number(s): 71.35.Ji, 71.70.Ej, 71.70.Gm

I. INTRODUCTION

The ordering of the crystal-field and spin-orbit coupling split states of the valence-band maximum in wurtzite ZnO has been the subject of controversy for more than 40 years. The nature of the valence-band maximum fine structure in ZnO was first studied by Thomas.[1] Based on the polarization dependence of the absorption and reflectivity spectra, he came to the conclusion that the valence-band ordering of ZnO is anomalous compared to the usual one in other II-VI wurtzite materials. Namely, the symmetry character of the highest valence-band state (leading to the so-called A exciton) according to his analysis is Γ_7 rather than Γ_9. The symmetry of the B state would then be Γ_9. The C exciton also has symmetry Γ_7. We will here label the states as A, B, and C from top to bottom, independent of their symmetry character. His interpretation was that the crystal-field splitting is large compared to the spin-orbit splitting. Without spin-orbit coupling, the valence band would be split into a singlet Γ_1 and a doublet Γ_5.[2,3] The singlet Γ_1 is essentially a p_z-like state (with slight s admixture) while the Γ_5 is a p_x,p_y-like state. With the usual $\Gamma_5>\Gamma_1$ ordering, one thus expects the C exciton to be allowed in $\mathbf{E}\|\mathbf{c}$ polarization and the Γ_5 derived (unresolved A,B excitons) to be allowed for the other polarization $\mathbf{E}\perp\mathbf{c}$. This is essentially what was observed in Thomas's reflectivity spectra. Absorption reveals the fine structure splitting in A and B excitons. With the spin-orbit coupling present, the Γ_7 state derived from the Γ_5 will obtain a slight admixture of p_z while the Γ_9 stays purely p_x and p_y like. Thus, one expects the Γ_7 state to become weakly allowed for $\mathbf{E}\|\mathbf{c}$. Thomas's data revealed this to be the case for the highest-energy A exciton: hence, his assignment. This was later confirmed by Liang and Yoffe.[4]

On the other hand, the interpretation of the lines by Thomas was challenged by Park *et al.*[5] They concluded on the basis of temperature dependence studies and on the basis of a prior study by Reynolds *et al.*[6] that the lines which were identified as the A-exciton lines A_m and A_L (the latter being a longitudinal exciton) by Thomas, in fact, did not arise from free-exciton states but corresponded to the Γ_5 and Γ_6 states of an ionized donor bound exciton. This was later disputed by other authors, among them by Segall,[7] who confirmed the free-exciton nature of the absorption line in question by a study of the phonon-assisted absorption onset. The controversy was never fully resolved, although most future papers adopted the interpretation of Thomas.

Recently, Reynolds *et al.*[8] restudied this issue using second-order photoluminescence spectra. The second order of the diffraction grating provided them higher resolution, fully resolving the additional fine structure of the excitons due to the exchange splitting. Furthermore, they studied the behavior of these spectra in a magnetic field. Their conclusion was that the line in question is indeed a free-exciton line, but that, nevertheless, the valence-band maximum must have Γ_9 symmetry. We will discuss their arguments below in more detail and show that they are based on assumptions about the sign of the Landé g factors, which we will later on in this paper show to be incorrect.

The ordering proposed by Thomas can be understood in terms of an effective negative spin-orbit splitting. The possibility of a negative spin-orbit splitting was first suggested by Cardona in a study of copper and silver halides.[9] It was subsequently explained by Shindo *et al.*[10] The origin is the presence of lower-lying d bands. The valence-band maximum being an antibonding combination of anion p-like states and cation d-like states results in a negative contribution of the atomic d orbitals to the effective spin-orbit splitting. Thus, one expects the possibility of a negative spin-orbit parameter

if the d bands lie fairly close to the valence-band maximum and have a strong atomic spin-orbit parameter. This is clearly the case in Cu compounds. The situation is marginal in ZnO, because the d bands here lie about 7 eV below the valence-band maximum (according to photoemission data.[11]) In previous work on the group-III nitrides, we pointed out the importance of the d bands in considerably reducing the values of the spin-orbit splittings[12] even though the d bands there lie even deeper than in ZnO.

In the present paper, we first present the results of a first-principles band structure calculation using the linearized muffin-tin orbital (LMTO) method[13,14] and carried out within the local density approximation[15] to the density functional theory. Spin-orbit coupling effects are included. These calculations indeed indicate a negative spin-orbit splitting and thus confirm Thomas' conclusion. From the above discussion, however, it is clear that the results of a negative spin-orbit splitting may depend crucially on the position of the d bands and the question arises whether the latter is obtained correctly in the local density approximation (LDA). We thus further investigate how shifts of the Zn $3d$ bands affect the conclusions of the valence-band ordering and show that it does not alter them for reasonable values of the shift.

We are then faced with a clear discrepancy between our theory and the most recent experimental data[8] or, at least, with the interpretation of those data given in the experimental paper. The comparison of our theory to the experimental data of Reynolds *et al.* is complicated by the fact that the experimentally observed features are excitons whereas we calculate valence bands. The question thus arises whether the ordering of the valence bands could possibly be different from the ordering of the corresponding exciton states due to differences in exciton binding energy of the excitons derived from each valence band or, more precisely, due to the interactions between these excitons. To address this question, a exciton fine structure calculation is carried out in the second part of the paper.

The method followed for that calculation has recently been fully described and applied to GaN.[16] In brief, a Kohn-Luttinger Hamiltonian[17,3] is taken as starting point and the electron-hole Coulomb interactions are added including the coupling between the excitons derived from different valence bands. The parameters in this model Hamiltonian are obtained as much as possible from our first-principles band structure and combined with some experimental data. The main conclusion of this part of the study is that the excitons follow the same ordering as the valence bands.

A careful analysis of the arguments used by Reynolds *et al.*[8] to arrive at their conclusions about the symmetry of the valence-band maximum reveals that it makes assumptions about the signs of the Landé g factor for the holes. The opposite conclusion, which would then be consistent with our present theory, would be obtained if the g factor for the holes involved in the A exciton were negative. In the final part of the paper, we show that this is indeed the case by a further elaboration of the Kohn-Luttinger model including the presence of a magnetic field. The splitting of the valence bands in a magnetic field is essentially determined by the Luttinger κ parameter. While this parameter was not calculated directly, we can determine it using a relation between κ and the Luttinger effective mass parameters[18] for the valence bands which are obtained from our first-principles band structure.

The remainder of the paper is organized as follows: first we describe the computational method used for the band structure calculations in Sec. II. Next, we describe the band structure results including a discussion of the Zn $3d$ band shift and our justification for the choice of this shift in Sec. III A. Using this same parameter, we then fit the bands to the Rashba-Sheka-Pikus (RSP) effective Hamiltonian and discuss the relationships between these parameters and the simplified Luttinger Hamiltonian used later in the paper in Sec. III B. In Sec. IV we briefly describe the exciton model Hamiltonian, including the magnetic field terms, describe its treatment by perturbation theory and give its results for the exciton binding energies in zero magnetic field. The fine structure due to the exchange terms and the results for the splitting in a magnetic field are presented in Sec. V. The differences between ours and the interpretation of Reynolds *et al.*[8] are also discussed in this section. The main conclusions are summarized in Sec. VI.

II. COMPUTATIONAL METHOD FOR BAND STRUCTURES

The basic computational framework used to determine the effective one electron potential of the band structure calculations is the density functional theory in the local density approximation.[15] We use the Hedin-Lundqvuist parametrization for the exchange-correlation potential.[19] Strictly speaking, the eigenvalues of the Kohn-Sham equation are not the quasiparticle eigenenergies but only intermediate results in the total energy calculation. However, the quasiparticle equation differs from the Kohn-Sham equation only in that the exchange correlation potential is replaced by a nonlocal and energy-dependent exchange-correlation self-energy operator. This leads to the well-known gap problem: the LDA underestimates the band gaps. It also leads to d bands that are too high in energy. This will be shown below to have repercussions for the valence-band splittings. We will discuss these effects beyond the LDA below along with the results. In this paper, we take the slightly empirical point of view of adjusting the Zn $3d$-band position so as to obtain good agreement with the splittings.

The linear muffin-tin orbital method[13] is used to solve the Kohn-Sham band structure equations. We used both the full-potential (FP) LMTO (Ref. 14) and the atomic sphere approximation (ASA). At present, the spin-orbit coupling is only incorporated in our ASA version of the computer code. The FP-LMTO results without spin-orbit coupling are found to be in good agreement with the corresponding ASA results. As usual for open structures, empty spheres are included to make the spheres close packed. The choice of empty spheres in wurtzite was described in detail in Kim *et al.*[20] We use the experimental lattice parameters $a=3.250$ Å, $c/a=1.6018$, and $u=0.382$. Well converged **k**-point sets were used for the Brillouin zone integrations in the self-consistent calculations. The spin-orbit coupling parameters derives primarily from

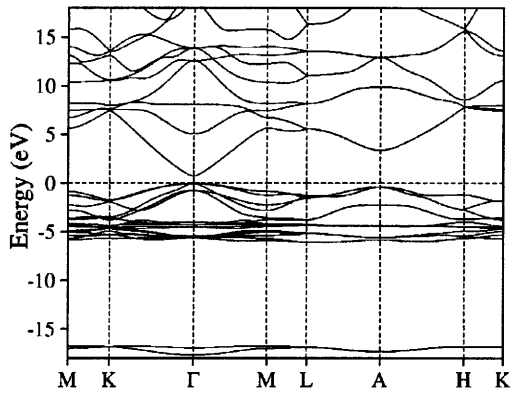

FIG. 1. Band structure of wurtzite ZnO in the local density approximation.

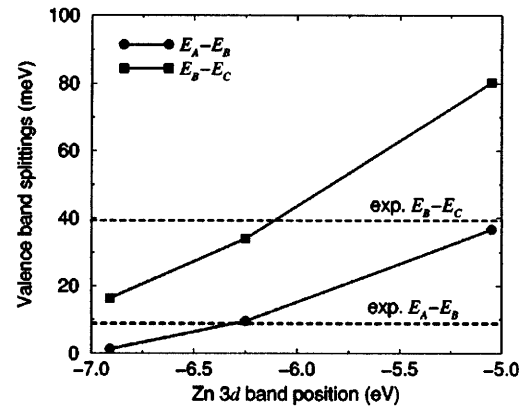

FIG. 2. Valence-band splittings vs Zn $3d$-band position in wurtzite ZnO.

regions well within the atomic sphere and thus the ASA is adequate for calculating its effects.

III. BAND STRUCTURE RESULTS

A. Band splittings at Γ

Figure 1 gives an overview of the band structure as obtained in the local density approximation and the FP-LMTO method and using experimental c/a and u values. In particular, we note the presence of the narrow Zn $3d$ bands at about -4 to -5 eV which play a crucial role in the present issue. While there is considerable dispersion and splittings of the d bands, we define a convenient d-band energy parameter by the weighted average of the d-derived bands at Γ. In the LDA this value is -5 eV. These results are comparable with other first-principles LDA calculations: for example, by Schröer *et al.*[21] and Xu and Ching.[22] However, these studies did not include the spin-orbit coupling effects and did not pay close attention to the valence-band maximum fine structure. The experimental value of the d-band position relative to the valence-band maximum measured by photoemission is -6.95 eV.[11]

The sign of the spin-orbit splitting was determined in two ways. First, we studied not only wurtzite ZnO but also zinc-blende ZnO. In zinc-blende ZnO, the valence-band maximum splits into a four-fold state of symmetry Γ_8 and a two-fold state of symmetry Γ_7. Simple inspection of the degeneracy of the eigenvalues revealed that the Γ_7 lies above the Γ_8, indicating a negative spin-orbit parameter. Second, inspection of the wave functions in the wurtzite case revealed that the highest valence band contains a p_z and s components, indicating Γ_7 symmetry while the second state had pure p_x,p_y (and some d admixture) but absolutely zero p_z or s components. This clearly means that in the LDA, a negative spin-orbit splitting is obtained, confirming Thomas' conclusion.

However, one may argue that the LDA calculation places the Zn $3d$ band too high in energy and thus overestimates the negative component of the spin-orbit splitting. We thus further investigated the behavior of the splitting as a function of d-band position. We can change the d-band position by simply adding a shift to the center of the Zn $3d$-band LMTO potential parameter $C_{\mathrm{Zn}\ 3d}$. These results are shown in Figs. 2 and 3. What we find is that both the crystal-field and spin-orbit splittings depend strongly on the d-band position. In fact, both decrease monotonically and nearly linearly as a function of increasing d-band binding energy. We find good agreement with the experimentally deduced E_A-E_B and E_B-E_C splittings for a d-band position of -6.25 eV. However, at the experimental d-band position, the crystal-field splitting is strongly underestimated. Next we attempt to explain this apparent paradox.

The origins of the discrepancy between the LDA and the photoemission results on the d-band position are twofold. First, there is the fact that the LDA treats exchange and correlation in an orbital independent manner and leads to a self-interaction error because of imperfect cancellation of the Coulomb and exchange integrals, in particular for localized states. Second, however, in the photoemission experiment, a final-state relaxation effect is involved. In some sense, in order to obtain the correct valence-band splitting we need to include the first but not the second effect.

Another way of phrasing this is within the language of many-body theory. The energy of a state as determined by

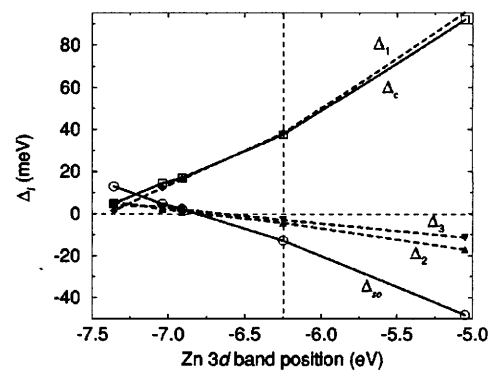

FIG. 3. Crystal-field ($\Delta_1=\Delta_c$) and spin-orbit splittings as function of Zn $3d$-band position: fits derived either with the quasicubic model using a single cubic Δ_{so} or with the anisotropic spin orbit parameters $\Delta_2=\Delta_{so}^{\parallel}/3$ and $\Delta_3=\Delta_{so}^{\perp}/3$ are shown.

photoemission is the quasiparticle energy, which follows from an equation which contains a nonlocal and energy-dependent self-energy operator instead of the exchange and correlation potential. This self-energy operator in the GW approximation[23,24] is essentially a dynamically screened Hartree-Fock exchange term. The energy dependence of this term implies that there is strictly no hope of correctly obtaining both the valence-band maximum (VBM) and the d-band states from the diagonalization of one energy-independent Hamiltonian matrix. On the other hand, let us assume that we make a static approximation to the screening of the exchange. In that case, we will already correct the self-interaction effect that the LDA gets wrong and obtain a much better orbital dependent treatment of exchange. Essentially, this will lead to a downward shift of the d band. This is what our calculation with shifted d-band potential parameter is simulating in a simple manner. Clearly, following the above argument we should not expect that we get the d band and VBM correct with the same shift. Thus, since we are here interested in the VBM, we adopt a slightly empirical point of view and use this shift as an adjustable parameter. That we obtain a d-band position intermediate between the LDA value and the experimental value for the correct VBM splitting is completely in agreement with expectations of the above outlined theory. Of course, a further *ab initio* justification of the d-band shift required would be preferable and is planned for future work. A simple way for correcting the spurious self-interaction of the d orbitals in II-VI's has been proposed within the framework of pseudopotentials by Vogel *et al.*[25]

The crystal-field splitting also depends sensitively on the crystal structure, in particular on the internal parameter u, which specifies the bond length $d=uc$ along the c axis. In the present calculations, we have used the experimental value $u=0.382$. FP-LMTO energy minimization calculations give a value very close to the experimental value $u=0.380$. For small enough changes, the crystal-field splitting increases linearly with increasing u and the deformation potential $d\Delta_c/d\ \ln u$ was calculated to be 2.7 eV, significantly smaller than in GaN.[26] One further expects that the gap underestimate of the LDA will overestimate the Γ_{1c}-Γ_{1v} interaction and thereby overestimate the crystal-field splitting. Opening the gap will therefore decrease the Δ_c. The ASA slightly underestimates the crystal-field splitting compared to the FP-LMTO and cancels some of the LDA error. As can be noticed from Figs. 2 and 3, the ASA with experimental u turns out to provide values in good agreement with experiment for both Δ_c and Δ_s for a reasonable and justifiable Zn $3d$-band shift.

As for the variation of the spin-orbit splitting with the Zn $3d$ band position, we note that this varies essentially linearly with the d-band contribution to the wave function (modulo squared) of the valence-band maximum. In fact, in a simple model,[10] $\Delta_s=\frac{3}{2}(-q_{\mathrm{Zn}\ 3d}\zeta_{\mathrm{Zn}\ 3d}+q_{\mathrm{O}\ 2p}\zeta_{\mathrm{O}\ 2p})$ with ζ_i the respective atomic spin-orbit coupling parameters and q_i the fractional contributions to the normalized wave function $|\psi_v|^2$. The atomic spin-orbit parameters are approximately[27] $\zeta_{\mathrm{Zn}\ 3d}=0.162$ eV, $\zeta_{\mathrm{O}\ 2p}=0.027$ eV; i.e., the Zn $3d$ atomic parameter is about a factor of 6 larger than the O $2p$ contribution. The contribution of the Zn $3d$ orbital to $|\psi_v|^2$ varies from about 21% to about 13% when going from the LDA to the shifted Zn $3d$-band position if we renormalize the wave function coefficients assuming only the O $2p$ and Zn $3d$ are present. These values indicate that qualitatively we are indeed close to the point of exact compensation of the two contributions to the spin-orbit coupling or close to the point where a sign change may occur. This simple model does not quite work quantitatively because we here neglect the Zn $4p$ contribution to the effective spin-orbit coupling and the fact that the values may differ slightly in the solid. Nevertheless, it provides some qualitative insight. The partial Zn $3d$ contribition to the normalization integral of the antibonding valence-band maximum state itself varies linearly with the Zn $3d$-band position as can be easily verified in a simple two-orbital-bond model and of course decreases as the Zn $3d$ is shifted down.

With the thus established Zn $3d$-band shift we examine again the symmetry of the VBM states. We find that we still have Γ_7 symmetry for the VBM. Also, if we use the same shift of the d band in zinc blende, we still find the doublet above the quartet. Finally, Fig. 3 shows that assuming a negative spin-orbit splitting at this d-band position leads to the expected nearly linear dependence versus the d-band position, whereas assuming a positive splitting would lead to a nonmonotonic behavior. Clearly, we can easily identify the point where the spin-orbit splitting passes through zero as a function of the d-band position. Furthermore, we note that if we shifted the d band to the point where the spin-orbit splitting becomes positive, the crystal-field splitting would be strongly underestimated. Further corrections beyond the LDA, in particular an upward shift of the conduction bands or gap correction, would be expected to slightly reduce the crystal-field splitting and thus would worsen the agreement if we assumed a positive spin-orbit splitting. This is because opening the gap would reduce the interaction of the Γ_1 with the conduction band and thus reduce the crystal field splitting. This effect is expected to be small. We note finally that with the optimal d-band shift obtained, the gap correction required for ZnO is similar to that in GaN. This is expected because the two materials have nearly the same experimental gap, as well as a close correspondence in lattice constant, density of electrons, and dielectric constant, all factors which influence the GW corrections. The only significant difference between the two is, in fact, the much closer-lying $3d$ bands in ZnO than in GaN.

In summary, there is no doubt that the calculation leads to a negative spin-orbit splitting even in a model that goes beyond the LDA by including the expected shifts of the d band and their influence on the crystal-field and spin-orbit splittings and gap correction.

For future reference, we provide in Table I the symmetry-labeled eigenvalues at Γ not only for the valence-band maximum but also for some of the higher conduction-band states and for the Zn $3d$ bands, which are relevant to $\mathbf{k}\cdot\mathbf{p}$ perturbation theory. No attempt is made at this time to obtain the valence-band parameters from perturbation theory. Instead we obtain them by direct fitting to the bands as discussed in the next section.

TABLE I. Eigenvalues at Γ in wurtzite ZnO.

Without spin orbit		With spin orbit		
Label	Energy (eV)	Label	Energy (eV)	Comment
Γ_1	−17.502	Γ_7	−17.507	O2s
Γ_3	−16.574	Γ_8	−16.580	
Γ_5	−6.719	Γ_9	−6.801	Zn3d
		Γ_7	−6.728	
Γ_1	−6.634	Γ_7	−6.589	
Γ_6	−6.583	Γ_9	−6.684	
		Γ_8	−6.487	
Γ_5	−6.003	Γ_7	−5.989	
		Γ_9	−5.971	
Γ_6	−5.760	Γ_8	−5.913	
		Γ_9	−5.681	
Γ_3	−5.738	Γ_8	−5.647	
Γ_3	−4.822	Γ_8	−4.815	O 2p
Γ_6	−0.710	Γ_9	−0.724	
		Γ_8	−0.706	
Γ_1	−0.039	Γ_7	−0.044	
Γ_5	0.000	Γ_9	−0.010	
		Γ_7	0.000	VBM
Γ_1	3.435	Γ_7	3.437	CBM[a]
Γ_3	7.101	Γ_8	7.126	
Γ_3	10.738	Γ_8	10.755	
Γ_5	16.005	Γ_7	15.924	
		Γ_9	16.117	
Γ_6	16.489	Γ_9	16.421	
		Γ_8	16.604	
Γ_1	16.634	Γ_7	16.675	
Γ_1	19.574	Γ_7	19.601	
Γ_5	21.283	Γ_7	21.286	
		Γ_9	21.395	
Γ_6	23.160	Γ_9	23.185	
		Γ_8	23.187	
Γ_3	24.430	Γ_8	24.436	
Γ_1	25.119	Γ_7	25.125	

[a]All calculated conduction bands are shifted up by 1.624 eV so as to agree with the experimental band gap of Ref. 8.

B. Effective mass parameters

Using the Zn 3d-band shift parameters determined above, we now examine the valence bands in the neighborhood of Γ and derive from them the Luttinger-type effective mass parameters. In fact, we here follow the procedure described in Kim *et al.*[26] The parameters of the 6×6 Rashba-Sheka-Pikus effective Hamiltonian[3] are adjusted so as to provide the best possible fit to the band structure for the highest six valence-band states (including the spin degree of freedom). The resulting parameters are given in Table II. Note that since we can in theory switch off the spin-orbit coupling at will, we obtain the crystal-field parameter Δ_c directly as the Γ_5-Γ_1 splitting. The three eigenstates at Γ, providing two energy differences, then allow us to obtain both the $\Delta_{so}^{\parallel}$ and $\Delta_{so}^{\perp}$ spin-orbit parameters from

TABLE II. Rashba-Sheka-Pikus Hamiltonian and related parameters: units $\hbar^2/2m_0$ for A_1–A_6 and γ_1–γ_3 with m_0 the free-electron mass and $e^2/2$ for A_7, meV for Δ_i, and m_0 for effective masses.

	A_1	A_2	A_3	A_4	A_5	A_6	A_7
	−3.78	−0.44	3.45	−1.63	1.68	−2.23	0.025
	Δ_c	$\Delta_{so}^{\parallel}$	$\Delta_{so}^{\perp}$	Δ_{so}^{cub}			
	38	−13.59	−9.15	−13			
	$m_{hh}^{\parallel}=m_{lh}^{\parallel}$[a]	$m_s^{\parallel}$	$m_{hh}^{\perp}$	$m_{lh}^{\perp}$	$m_s^{\perp}$		
	3.06	0.26	2.59	0.30	1.12		
	$m_A^{\parallel}$[b]	$m_A^{\perp}$	$m_B^{\parallel}$	$m_B^{\perp}$	$m_C^{\parallel}$	$m_C^{\perp}$	
Present	2.74	0.54	3.03	0.55	0.27	1.12	
Expt.[c]	0.59	0.59	0.59	0.59	0.31	0.55	
$\mathbf{k}\cdot\mathbf{p}$[d]	0.67	0.63	0.67	0.63	0.25	2	
K-L[e]	2.16	0.48	2.33	0.47	0.27	2.24	
K-L[f]	2.74	0.49	3.03	0.48	0.26	2.88	
	γ_1[g]	γ_2	γ_3	κ			
set 1	1.55	0.56	0.56	−0.25			
set 2	1.49	0.58	0.58	−0.20			

[a]Effective masses in the absence of spin-orbit coupling.
[b]Effective masses including spin-orbit coupling.
[c]Ref. 28.
[d]Ref. 29.
[e]From quasicubic Kohn-Luttinger model with parameter set 1.
[f]From quasicubic Kohn-Luttinger model with parameter set 2.
[g]Quasicubic Kohn-Luttinger parameters; see text.

$$E_{\Gamma_9}-E_{\Gamma_7}=\frac{1}{2}\left[\Delta_c+\Delta_{so}^{\parallel}\pm\sqrt{\left(\Delta_c-\frac{\Delta_{so}^{\parallel}}{3}\right)^2+\frac{8}{9}\Delta_{so}^{\perp 2}}\right]. \tag{1}$$

The − sign corresponds to the upper Γ_7 or BA splitting, the + sign to the lower Γ_7 or BC splitting. These energy differences are labeled Δ_1 and Δ_2 in Ref. 16. Note that in Ref. 26, Δ_c is called Δ_1, $\Delta_{so}^{\parallel}$ corresponds to $3\Delta_2$, and $\Delta_{so}^{\perp}$ corresponds to $3\Delta_3$. The inverse mass parameters A_1–A_6 are obtained by first fitting parabolic curves to the bands in the directions parallel and perpendicular to the c axis and by using the analytic expressions relating the effective masses and the A_i parameters given in Eq. (7) of Ref. 26. The linear-in-**k** A_7 parameter, which is related to the anticrossing of the light-hole and split-off hole band in the perpendicular direction, is obtained by adjusting the parameter to the resulting nonparabolicity of the bands. Finally, the parameters are fine-tuned to give the best overall fit over a range of **k** values. The first-principles energy levels of approximately 1700 **k** points within a sphere of radius of $0.07\times 2\pi/a$ centered at Γ in **k** space were used in the fittings. This is to ensure the overall (not just in some specific directions) fit of the RSP parameters. Figure 4 illustrates the quality of the fit. The average root-mean-square deviation of the fitted and first-principles energies is less than 3 meV. We note that the spin splitting of the bands in the perpendicular direction is not completely accurately reproduced by the model. This indicates the need for further linear in **k** terms in the Hamil-

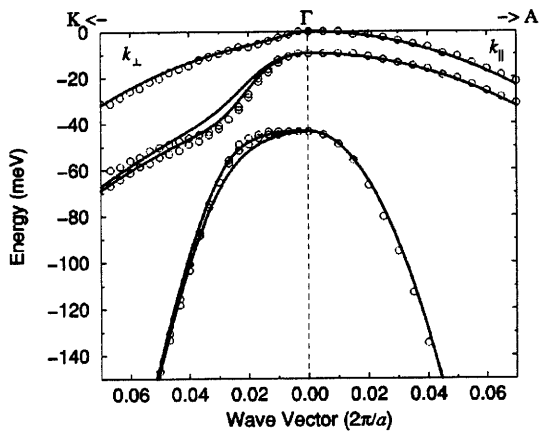

FIG. 4. Band structure of ZnO. The open circles represent the ASA-LMTO results including spin-orbit coupling. The solid lines represent the RSP fit.

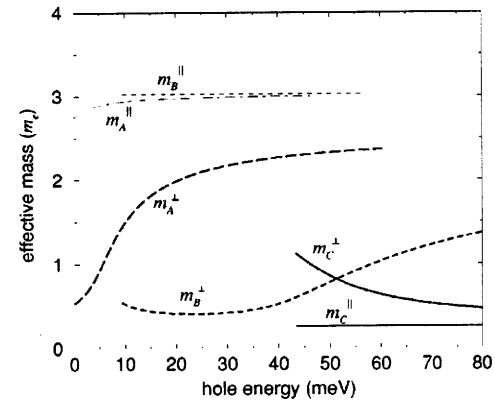

FIG. 5. Energy-dependent effective hole masses: thick lines, $k_\perp$; thin lines, $k_\parallel$.

tonian which are of relativistic origin and denoted by α_i in Ref. 26. Since here we are primarily interested in deducing an even simpler Kohn-Luttinger model, we did not attempt to fit the α_i terms. We also investigated the sensitivity of these parameters to the Zn $3d$-band position. The A_1–A_7 parameters vary basically linearly with the d-band position and change by a few % when going from the LDA to the optimal d-band location identified above. The effective masses differ significantly when spin-orbit coupling is included from those when it is neglected. Also, the effective mass of the split-off hole band in the perpendicular direction is strongly affected by the band anticrossing effect. Our values are in reasonable agreement with the experimental values of Hümmer[28] except for $m_A^\parallel$ and $m_B^\parallel$ and $m_C^\perp$. The reason for these discrepancies is not clear. We only remark that the experimental values are deduced from a somewhat elaborate analysis of the behavior of Landau levels measured by magnetoreflection in which the Coulomb effects are only treated crudely. We also compare our results with those obtained by $\mathbf{k}\cdot\mathbf{p}$ theory.[29]

The combined effect of the spin-orbit splitting at Γ with the various interactions between the bands leads to significant nonparabolic behavior of the bands. We can describe this in terms of energy-dependent masses as in Ref. 26. The resulting energy-dependent masses are shown in Fig. 5. We note in particular the strong energy dependence of the $m_A^\perp$.

In Sec. IV and V, a simplified quasicubic Kohn-Luttinger model is adopted in order to facilitate the exciton calculations. It is thus of interest to investigate how well the quasicubic model works. The relations between the RSP parameters and the quasicubic parameters A,B,C were given in Eq. (5) of Kim *et al.*[26] Furthermore, the Luttinger parameters are

$$\gamma_1 = -(A+2B)/3,$$
$$\gamma_2 = -(A-B)/6,$$
$$\gamma_3 = -C/6. \tag{2}$$

From $-6\gamma_3 = C = -A_3 = 2A_4$, we obtain $\gamma_3 = 0.56 \pm 0.02$. From $A_1 = -\gamma_1 - 4\gamma_3$ and $A_2 = -\gamma_1 + 2\gamma_3$, we obtain $\gamma_1 = 1.55 \pm 0.01$ and, finally, from $A_5 = \gamma_2 + 2\gamma_3$, we obtain $\gamma_2 = 0.56$. Thus, the axial model with a single $\gamma = \gamma_2 = \gamma_3$ appears to be well applicable for ZnO. On the other hand, solving the two equations $(\gamma_1 - 2\gamma_3) = -(A_1 + A_3)$ and $(\gamma_1 + \gamma_3) = -(A_2 + A_4)$ for γ_1 and $\gamma_3 = \gamma$ gives $\gamma_1 = 1.49$ and $\gamma = 0.58$. Thus, there is some uncertainty simply from the fact that we try to reduce a six-parameter model to a two-parameter model and the choice of equations to use is not unique. To gauge the effect of this uncertainty on the results of the calculations, we have used two sets for (γ_1, γ): (1.55,0.56) and (1.49,0.58). The corresponding values of the effective masses obtained using Eqs. (10)–(12) in Ref. 16, but with A and B interchanged because A in GaN corresponds to Γ_9 while here it corresponds to Γ_7, are also included in Table II.

For the excitonic calculations below, we also need the conduction-band electron masses. For the latter we obtain

$$m_e^\parallel = 0.23 m_0, \quad m_e^\perp = 0.21 m_0, \tag{3}$$

by direct fitting to the first-principles bands with the same d-band shift applied as before. Here, m_0 is the bare electron mass. These values are expected to be slight underestimates because of the underestimate of the gap. The bare mass as obtained from a Faraday rotation measurement is $0.24 m_0$.[30] The polaronic mass was determined to be $0.28 m_0$ for $\mathbf{H} \| \mathbf{c}$ and $0.24 m_0$ for $\mathbf{H} \perp \mathbf{c}$ by cyclotron resonance measurements of Button *et al.*[31]

IV. EXCITON BINDING ENERGIES

The Hamiltonian for the relative motion of the exciton in a magnetic field in a hexagonal semiconductor is

$$\hat{H}_{exc}(\mathbf{r}) = \hat{H}_e\left(-i\nabla + \frac{e}{\hbar c}\mathbf{A}\right) - \hat{H}_h\left(i\nabla + \frac{e}{\hbar c}\mathbf{A}\right) - \frac{e^2}{\sqrt{\varepsilon_0^\parallel \varepsilon_0^\perp (x^2+y^2) + \varepsilon_0^{\perp 2} z^2}}, \tag{4}$$

where $(x,y,z) = (\mathbf{r})$ are the relative electron-hole coordinates (the z direction is chosen along the hexagonal c axis), e is the

magnitude of the free-electron charge, $\varepsilon_0^{\parallel}$ and $\varepsilon_0^{\perp}$ are the low-frequency dielectric constants, and $\mathbf{A}=(1/2)[\mathbf{H}\times\mathbf{r}]$ is the vector potential of the magnetic field. We write the kinetic energy parts of both the electron, $\hat{H}_e$, and the hole, $\hat{H}_h$, effective envelope Hamiltonians in the quasicubic approximation,[3] neglecting relativistic terms linear in $\hat{\mathbf{k}}=\mp i\nabla+e\mathbf{A}/\hbar c$, respectively, as

$$\hat{H}_e(\hat{\mathbf{k}})=\frac{\hbar^2}{2m_e^{\parallel}}k_z^2+\frac{\hbar^2}{2m_e^{\perp}}(k_x^2+k_y^2)+\frac{1}{2}g_e^{\parallel}\mu_B(\hat{\sigma}_z H_z)+\frac{1}{2}g_e^{\perp}\mu_B(\hat{\sigma}_x H_x+\hat{\sigma}_y H_y), \tag{5}$$

$$-\hat{H}_h(\hat{\mathbf{k}})=\frac{\hbar^2}{2m_0}\left[(\gamma_1+4\gamma)k^2-6\gamma\left(\sum_{\alpha=x,y,z}k_\alpha^2\hat{I}_\alpha^2+2\sum_{\alpha\neq\beta}\{k_\alpha k_\beta\}\{\hat{I}_\alpha\hat{I}_\beta\}\right)\right]-\frac{1}{3}\Delta_{so}^{\parallel}[(\hat{I}_z\hat{\sigma}_z)-1]-\frac{1}{3}\Delta_{so}^{\perp}(\hat{I}_\perp\hat{\sigma}_\perp)-\Delta_c[\hat{I}_z^2-1]-\mu_B(1+3\kappa)(\hat{\mathbf{I}}\mathbf{H})+\frac{1}{2}\mu_B g_0(\hat{\sigma}\,\mathbf{H}), \tag{6}$$

where $g_0=2, g_e^{\parallel}, g_e^{\perp}$ are the free-electron and conduction-band parallel and perpendicular g factors, respectively, $\mu_B=e\hbar/2m_0c$ is the Bohr magneton, $\hat{\sigma}_{x,y,z}$ are the Pauli matrices, $\hat{\mathbf{I}}$ is the orbital angular momentum operator of the hole ($I=1$), $\{ab\}=(ab+ba)/2$, and κ is the magnetic Luttinger constant.[17]

To calculate the free-exciton energy levels from the Hamiltonian of Eq. (4) we first rescale the coordinates $x\to x$, $y\to y$, and $z\to z\sqrt{\eta}$, where $\eta=\varepsilon_0^{\perp}/\varepsilon_0^{\parallel}$. This leads to a separation into isotropic and anisotropic terms as well as coupling terms. If the latter two are neglected, the problem reduces to the hydrogenic problem for the envelope function. Under suitable conditions, which we will show below to be satisfied here, the anisotropy and coupling terms as well as the magnetic field terms can be treated in second-order perturbation theory following the approach of Baldereschi, Lipari, and Altarelli[32,33] as fully described in Ref. 16. The important parameters for the validity of the perturbation treatment are $p_\upsilon=\mu_\upsilon/\mu_\upsilon^{an}$, with $\upsilon=A,B,C$ and $p_h=\gamma\mu_0/m_0$, defined below and which are, respectively, a measure of the anisotropy and coupling. The coupling terms further involve the dielectric constant anisotropy factor η defined earlier and the mixing parameters of the various Bloch basis functions of the valence-band edge in the spin-orbit coupled states,

$$u_B^{+}=|1,1\rangle\uparrow,\quad u_B^{-}=|1,-1\rangle\downarrow,$$
$$u_A^{+}=ia|1,1\rangle\downarrow-ib|1,0\rangle\uparrow,\quad u_A^{-}=a|1,-1\rangle\uparrow+b|1,0\rangle\downarrow,$$
$$u_C^{+}=ib|1,1\rangle\downarrow+ia|1,0\rangle\uparrow,\quad u_C^{-}=b|1,-1\rangle\uparrow-a|1,0\rangle\downarrow, \tag{7}$$

with $|l,m\rangle$ the usual spherical harmonics or angular momentum eigenstates, $|1,\pm1\rangle=(|X\rangle\pm i|Y\rangle)/\sqrt{2}$, $|1,0\rangle=|Z\rangle$.

The a and b mixing coefficients are derived from the knowledge of the crystal-field and spin-orbit splittings, in terms of

$$a=\frac{1}{\sqrt{x^2+1}},\qquad b=\frac{x}{\sqrt{x^2+1}},$$

$$x=\frac{-(3\Delta_c-\Delta_{so}^{\parallel})+\sqrt{(3\Delta_c-\Delta_{so}^{\parallel})^2+8\Delta_{so}^{\perp\,2}}}{2\sqrt{2}\Delta_{so}^{\perp}}. \tag{8}$$

The values of a and b are 0.9950 and -0.0999.

Another important factor, affecting the ground $1S$ and excited $2S$ exciton state energies, is the polar interaction of excitons with optical phonons. The exact description of the exciton–optical-phonon system in wurtzite semiconductors such as ZnO and GaN has not been developed. To estimate the "polaron" effects we use here the simple band isotropic Pollmann-Büttner model[34] as described in Ref. 16. For this, we add to the isotropic part of the Coulomb interaction potential, $-e^2/\varepsilon_0 r$, where $\varepsilon_0=\sqrt{\varepsilon_0^{\parallel}\varepsilon_0^{\perp}}$, the Pollmann-Büttner correction potential V_{PB}^{pol} given by

$$V_{PB}^{pol}=-\frac{e^2}{\varepsilon^{pol}r}\frac{1}{\Delta m}\left[m_h\exp\left(-\frac{r}{l_h}\right)-m_e\exp\left(-\frac{r}{l_e}\right)\right]. \tag{9}$$

Here $1/\varepsilon^{pol}=(1/\varepsilon_\infty-1/\varepsilon_0)$; $\varepsilon_\infty=\sqrt{\varepsilon_\infty^{\parallel}\varepsilon_\infty^{\perp}}$; m_e and m_h are the electron and hole effective masses, respectively, averaged over the three directions in $\mathbf{k}$ space, $1/m_e=(2/m_e^{\perp}+1/m_e^{\parallel})/3$ and $1/m_h=\gamma/m_0$ (note that m_h is the same for all valence subbands); and $\Delta m=m_h-m_e$, and $l_{e,h}=\sqrt{\hbar^2/2m_{e,h}E_{LO}}$ are the electron- and hole-polaron radii. The energy of optical phonons in ZnO is known to be[35] $E_{LO}=72$ meV, and the values used for the low-frequency, $\varepsilon_0^{\parallel,\perp}$, and high-frequency, $\varepsilon_\infty^{\parallel,\perp}$, dielectric constants are[36]

$$\varepsilon_0^{\parallel}=8.49,\quad \varepsilon_0^{\perp}=7.40, \tag{10}$$

$$\varepsilon_\infty^{\parallel}=3.72,\quad \varepsilon_\infty^{\perp}=3.68. \tag{11}$$

According to Pollmann and Büttner,[34] the "bare" band electron and hole effective mass parameters are used in the Hamiltonians of Eqs. (5) and (6) as well as in Eq. (9). The correction potential of Eq. (9) is treated as a perturbation on the same basis as the anisotropic and coupling terms described in Ref. 16.

We will focus only on the ground $n=1$ and excited $n=2$ exciton states of the S symmetry and present the resulting exciton transition energies in zero magnetic field as

TABLE III. Binding energy contributions to the $1S$ and $2S$ excitons, all energies in meV.

v	R_v	ΔE_v^{an}	ΔE_v^{coup}	ΔE_v^{pol}	E_v^{bind}	ΔE_v^{12}
			$1S$ excitons			
A	36.25	0.58	1.67	11.45	49.94	
B	36.24	0.60	2.06	11.44	50.33	
C	37.12	0.64	3.00	11.72	52.49	
			$2S$ excitons			
A		0.90	1.80	2.28	10.31	39.63
B		0.93	2.05	2.28	10.37	39.96
C		1.00	0.84	2.33	10.32	42.16

[a] $\Delta E_v^{12}=E_{v,1}^{bind}-E_{v,2}^{bind}$.

$$E_{v,n}^{0}=E_v^g-E_{v,n}^{bind}, \tag{12}$$

where E_v^g is the separation between the bottom of the conduction band and the top of each of the $v=A,B,C$ valence subbands and the binding energies are given by

$$E_{v,n}^{bind}=\frac{1}{n^2}(R_v+\Delta E_{v,n}^{an}+\Delta E_{v,n}^{coup}+\Delta E_{v,n}^{pol}). \tag{13}$$

The effective Rydbergs $R_v=\mu_v e^4/2\hbar^2\varepsilon_0^2$ are calculated with the exciton reduced masses μ_v averaged over the three directions in $\mathbf{k}$ space: $1/\mu_v=(2/\mu_v^{\perp}+\eta/\mu_v^{\parallel})/3, 1/\mu_v^{\perp,\parallel}=1/m_v^{\perp,\parallel}+1/m_e^{\perp,\parallel}$. The terms $\Delta E_{v,n}^{an}$, $\Delta E_{v,n}^{coup}$ and $\Delta E_{v,n}^{pol}$ contain the anisotropy, intersubband coupling, and polaron corrections, respectively, calculated in the second order of perturbation theory. We note that the indices A and B in all expression given in Ref. 16 for GaN must be inverted when applied to ZnO due to the inverse order of the upper Γ_7 and Γ_9 subbands.

To examine the effects of the uncertainty of the Kohn-Luttinger parameters, we carried out the calculations with four sets of parameters. The first set uses $\gamma_1=1.55, \gamma=0.56$, and the electron masses of Eq. (3). In the second set, the same γ's but an isotropic electron mass of 0.24 are employed. The third and fourth sets use $\gamma_1=1.49, \gamma=0.58$ with electron masses of Eq. (3) and 0.24, respectively.

The perturbation parameters $p_v=\mu_v/\mu_v^{an}$, where $1/\mu_v^{an}=(1/\mu_v^{\perp}-\eta/\mu_v^{\parallel})/3$ for anisotropic corrections, and $p_h=\gamma\mu_0/m_0=\mu_0/m_h$, where $1/\mu_0=(1/\mu_A+1/\mu_B+1/\mu_C)/3$ for the coupling corrections, obtained with the first set are $p_h=0.095$, $p_A=0.149$, $p_B=0.151$, and $p_C=0.155$. Similar values are obtained with the other sets of parameters. All are about 0.1, showing that perturbation theory is well satisfied. In particular, for the $1S$ states all expressions involve the square of these parameters.

In Table III we provide the different components of the binding energy for the $1S$ and $2S$ states as calculated with the first set of parameters. For the $2S$ states we also give $\Delta E_v^{12}=E_{v,1}^{bind}-E_{v,2}^{bind}$. Because the other parameter sets produce very similar results, we do not give the results explicitly but only discuss the trends. First of all, we note that the anisotropy and coupling contributions are relatively small compared to the effective Rydberg and the polaron correction. Next, we note that the binding energy differences between the A and B and between the B and C excitons are less than 1 meV and 2 meV, respectively. These are small compared to the A-B and B-C splittings. Using a somewhat larger electron mass of 0.24 leads to an increase in binding energy of about 5–6 meV for the $1S$ states, of which 3 meV is due to the change in the effective Rydberg, 2 meV, due to the polaron correction, and 0.5 meV due to the coupling contributions. It leads to an increase in binding energy of the $2S$ states by only 1 meV. The alternative set of Kohn-Luttinger parameters (used in sets 3 and 4) tends to increase the anisotropy and coupling corrections by less than 1 meV.

The substantial corrections to the Rydberg imply that the exciton binding energies cannot be directly obtained from the experimental separation between $n=1$ and $n=2$ states, ΔE_v^{12} by the simple relation $4/3\Delta E_v^{12}$. For example, using set 1 we obtain for the energy separation between $1S$ and $2S$ energy levels 39.63 meV for the A exciton and 39.96 meV for the B exciton. These values differ significantly from $3/4E_{A,1}^{bind}$ and $3/4E_{B,1}^{bind}$, respectively. They can also be compared with 3/4 of the binding energies reported in Ref. 8: 60.0 meV for A excitons and 57.0 meV for B excitons, which give $\Delta E_v^{12}(A)=45.0$ meV and $\Delta E_v^{12}(B)=42.75$ meV, respectively.

Overall, the agreement with the binding energies deduced from the experiment are fairly good, given that no parameters were adjusted to the binding energies, all parameters being derived either from theory or from other experimental data, and keeping in mind the above-mentioned difficulties in extracting binding energies directly from the splittings of excited and ground states of the excitons. In addition, the treatment of the numerically important polaron effect used here should be considered as a fairly rough estimation. In any case, the conclusions about the order of the A, B, and C exciton ground-state transition will not change if one uses more elaborate polaron models.

The main conclusion of this section is thus that the excitons closely maintain their principal valence-band character even when band mixing effects are included. The binding energy differences are small compared to the valence band-splittings. In other words, the lowest energy exciton is still the one primarily derived from the top valence band, i.e., from the Γ_7 valence band, even when coupling effects are included.

V. EXCHANGE AND MAGNETIC FIELD EFFECTS

The electron-hole exchange interaction is not included in the exciton Hamiltonian considered so far. It contains both short-range and long-range contributions[37–39] or, as some authors prefer, analytic and nonanalytic terms.[40–42] The short-range part can be written in the form

$$H_{ex}=\frac{J_{SR}}{2}(1-\boldsymbol{\sigma}_h\cdot\boldsymbol{\sigma}_e). \tag{14}$$

The effect of the long-range terms can be incorporated by replacing J_{SR} by an effective J_K, which depends on the wave vector of the exciton translation motion and is different for longitudinal excitons, i.e., $\mathbf{K}\|\boldsymbol{\mu}$ with $\boldsymbol{\mu}$ the dipole moment of the exciton and transverse excitons. Following Skettrup and Balslev,[39] we can write

$$J_L = J_{SR} + \frac{2}{3} J_{LR},$$

$$J_T = J_{SR} - \frac{1}{3} J_{LR}. \tag{15}$$

The possible symmetries of the exciton states derived from the symmetries of the valence and conduction bands at Γ are

$$\Gamma_7 \otimes \Gamma_7 = \Gamma_1 \oplus \Gamma_2 \oplus \Gamma_5,$$

$$\Gamma_9 \otimes \Gamma_7 = \Gamma_6 \oplus \Gamma_5. \tag{16}$$

Only Γ_5 for $\mathbf{E}\perp\mathbf{c}$ and Γ_1 for $\mathbf{E}\|\mathbf{c}$ correspond to allowed transitions. The other lines are forbidden but may still be weakly visible because the finite $\mathbf{k}$ contribution in the exciton states or because of imperfect alignment of the beams with respect to the crystal axis. The Γ_5 states correspond to a total (spin+orbital) angular momentum projection $J_{tot,z}$ of the hole and electron equal to ± 1. For the $\Gamma_9 \otimes \Gamma_7$ derived states, they are formed by $u_v^+ u_e^-$ and $u_v^- u_e^+$, with the electron states $|u_e^+\rangle = |s\rangle\uparrow, |u_e^-\rangle = |s\rangle\downarrow$ and the hole states defined in Eq. (7). In other words, they are the combinations of the $J_{hz} = \pm 3/2$ states of the hole with the $J_{ez} = \pm 1/2$ states of the electron, giving rise to a total momentum projection of $J_{tot,z} = \pm(|J_{hz}| - |J_{ez}|) = \pm 1$, and have antiparallel electron and hole spins. The Γ_6 states are constructed from the products of the same electron and hole states but with the electron spins interchanged. Here the electron spins are thus parallel to those of the holes. The $\Gamma_7 \otimes \Gamma_7$ derived Γ_5 corresponds to the $u_v^+ u_e^+$ and $u_v^- u_e^-$ functions, corresponding to the sum of electron and hole total momenta, $J_{ez} = \pm 1/2$ and $J_{hz} = \pm 1/2$, leading to $J_{tot,z} = \pm(|J_{ez}| + |J_{hz}|) = \pm 1$. For the upper Γ_7 state ($v = A$) which has mainly xy character [in fact, see Eq. (8), $a = 0.995$], the Γ_5 exciton again corresponds to a state with mainly antiparallel electron and hole spins. The Γ_1 and Γ_2 exciton states are constructed from products of the same band states but with the electron states interchanged. The dominant components of these states have parallel electron and hole spins. They would be Kramers degenerate if the interaction with the crystal-field split-off band were neglected. In practice they are still very nearly degenerate. Only the states with antiparallel electron and hole spins are affected by the exchange Hamiltonian, as written in Eq. (14). Due to the additional long-range effects, the $\Gamma_{5(T,L)}$ states are effectively shifted upwards by $J_{(T,L)}$ with respect to the Γ_1 and Γ_2 states. The exchange Hamiltonian also leads to off-diagonal terms between the different Γ_5 states.

Since the Hamiltonian of Eq. (4) does not contain the exchange term, the results for the binding energies given in the Table III strictly speaking pertain to the (Γ_1, Γ_2) and Γ_6 states for the A and B excitons, respectively. In order to experimentally identify these different symmetry states, it is useful to consider their behavior in a magnetic field. We do that next.

For a sufficiently weak magnetic field, the corresponding terms in the Hamiltonian can be treated by perturbation theory at the same level as the anisotropy and exciton coupling terms. The Zeeman energy for the electrons is $\pm 1/2 \mu_B g_e^{\|,\perp} H^{\|,\perp}$ for the magnetic field $H^{\|}$ directed parallel and $H^{\perp}$ directed perpendicular to the c axis, and "+" (in parallel field) is for the spin up state u_e^+. The reported values for the anisotropic g tensor are in the ranges[43,44]

$$g_e^{\|} = 1.956\text{–}1.958, \quad g_e^{\perp} = 1.955\text{–}1.956. \tag{17}$$

The g tensors for the various valence bands are all expressed in terms of the single κ constant in Ref. 16, Eqs. (30)–(32). The latter is obtained from the well-known relationship[18]

$$\kappa = (-2 - \gamma_1 + 5\gamma)/3, \tag{18}$$

for which we obtain the value $\kappa = -0.25$ with the γ set 1 and -0.197 with γ set 2 as considered before. If $\mu_B H$ is small compared to the valence-band splittings Δ_1 and Δ_2, the Zeeman energy for valence subbands is $\pm 1/2 \mu_B g_v^{\|,\perp} H^{\|,\perp}$, where again the "+" sign in parallel field corresponds to the positive projection of the hole total momentum: i.e., the u_v^+ function.

For the free holes in the A, B, and C valence subbands we obtain

$$g_A^{\|} = -2.455(-2.772), \quad g_A^{\perp} = 0.09(0.135), \tag{19}$$

$$g_B^{\|} = 1.50(1.18) \quad g_B^{\perp} = 0(0), \tag{20}$$

$$g_C^{\|} = 1.955(1.952), \quad g_C^{\perp} = 1.91(1.865), \tag{21}$$

in which the values in parentheses correspond to the κ value of -0.197 and the other to $\kappa = -0.25$

In Ref. 16, it is shown that the perpendicular values are not affected by the coupling effects and are the same for the holes involved in any exciton states. On the other hand, the values of the parallel g factor of the holes involved in the exciton states are affected significantly by the coupling between excitons belonging to the different valence subbands and might be very different from the free hole g values and for the hole in different exciton states. Recently, the effect of different g values for the free hole and the hole involved in the $1S$ exciton state in the $A(\Gamma_9)$ subband in wurtzite GaN has been observed experimentally.[45]

With the parameters described above we obtain for the hole g values in the ground $1S$ states of A, B, and C excitons the values given in Table IV for the four sets of parameters investigated. We may note that the g values are a bit more sensitive to the choice of parameters than are the binding energies. The differences due to the different parameter sets are of the same magnitude as the differences between the different experimental reports, also included in Table IV.

TABLE IV. Effective Landé g factors for the holes participating in $1S$ excitons.

	$g_A^{\parallel}(1S)$	$g_B^{\parallel}(1S)$	$g_C^{\parallel}(1S)$
Set 1	−1.335	3.038	1.062
Set 2	−1.227	3.145	1.130
Set 3	−1.556	2.843	1.445
Set 4	−1.438	2.961	1.178
Ref. 8	|1.2|		
Ref. 28	|1.7|		
Ref. 47	|1.6|	|1.95|	
Ref. 48	|1±0.5|	|2.7±0.5|	

Using these values we can finally calculate the $1S$ exciton effective g factors for the states of different symmetry. For the $A(\Gamma_7\otimes\Gamma_7)$ exciton we have for the Γ_5 state $g_e^{\parallel}+g_A^{\parallel}(1S)\approx 0.4$–$0.7$ and for the Γ_1-Γ_2 Zeeman splitting $g_e^{\parallel}-g_A^{\parallel}(1S)\approx 3.3$–$3.5$, the range of values being due to the uncertainty in the parameters. Note that the Γ_2 exciton is forbidden without a magnetic field but becomes allowed in a magnetic field because the latter has symmetry Γ_2. The Γ_1 and Γ_2 states, which are nearly degenerate without a magnetic field, then couple and repel each other, resulting in the splitting. The relevant g factors just deduced have to be compared with the value 3.09 reported by Reynolds *et al.*[8] for the Zeeman splitting of the exciton ground state at 3.3756 eV. They obtained a negligible splitting for the higher-energy A exciton at 3.3773 eV, which is compatible with our Γ_5 exciton g factor being less than 1.

Our assignment of the lines is in agreement with that by Thomas[1] but differs from that of Reynolds *et al.*[8] Their assignment differs from ours primarily because they assumed a positive g_v factor for the hole. Note that for the $\Gamma_7\otimes\Gamma_7$ derived Γ_5 exciton the effective splitting is given by $|g_e+g_v|$ whereas for the $\Gamma_9\otimes\Gamma_7$ derived Γ_5 exciton, the effective splitting is given by $|g_e-g_v|$. Thus, with a positive g_v and g_e the small splitting of the Γ_5 state indicated to them that this exciton would be Γ_9 derived. However, the present calculations shows that with a Γ_7 VBM, the g_v for the A exciton is negative and thus the sum of the g factors becomes negligible. Furthermore, our value for the Γ_1-Γ_2 Zeeman splitting is in good agreement with the data. A negative g factor was reported previously for the Γ_7 valence band in GaN by Campo *et al.*[46]

For the $B(\Gamma_9\otimes\Gamma_7)$ exciton we have for the Γ_5 state $|g_e^{\parallel}-g_B^{\parallel}(1S)|\approx 0.9$–$1.1$ and for the Γ_6 splitting $g_e^{\parallel}+g_B^{\parallel}(1S)\approx 4.9$–$5.1$. The values for the B-exciton g factors predicted here are significantly larger than the values reported by Blattner *et al.*[47] obtained from two-photon Raman scattering. This discrepancy requires further study. The g factors for the A exciton reported by these authors are somewhat larger than those reported by Reynolds *et al.*[8] and closer to the upper range of values obtained with parameter sets 3 and 4. It should be noted that Blattner *et al.*[47] obtained conflicting results from reflection and absorption data for the g splittings of the B exciton. So further experimental study of the behavior of the B exciton in a magnetic field would be worthwhile. Our results compare best of all with the most recent data of Rosenzweig.[48]

Returning to the experimental data of Reynolds *et al.*,[8] one might ask why, within our current interpretation, the Γ_1 is so weak compared to Γ_5 for $\mathbf{E}\|\mathbf{c}$. One might further argue that in luminescence the low-energy excitation should appear stronger because of the Boltzmann occupation factor. However, it should be kept in mind that this state still is primarily x,y like with only a very small z admixture because the crystal-field splitting is much larger than the spin-orbit splitting. Thus, it is intrinsically a weak transition even if allowed.

Second, we note that the peak at 3.3773 eV in the $\mathbf{E}\|\mathbf{c}$ spectrum corresponds to the longitudinal exciton.[49] This interpretation is confirmed by the studies of Blattner *et al.*,[47] Kuhnert *et al.*,[50] and Hümmer *et al.*[51] According to these papers, the Γ_{5T} state is much closer to the Γ_1 state. The Γ_{5L}-Γ_1 splitting of 1.7 meV does not directly give the exchange interaction parameter J_L because of the presence of off-diagonal matrix elements of the exchange interaction Hamiltonian between the $\Gamma_9\otimes\Gamma_7$ and $\Gamma_7\otimes\Gamma_7$ derived Γ_5 states. From the paper of Skettrup and Balslev,[39] we extract a Γ_{5L}-Γ_1 splitting of 2.2 meV and a Γ_{5T}-Γ_1 splitting of 0.8 meV in fairly good agreement with the above assignments. The values used in their analysis for the exchange parameters correspond to $J_L=13.4$ meV and $J_T=1.8$ meV. We then obtain $J_{SR}=5.7$ meV and $J_{LR}=11.7$ meV. This should be compared with the exchange parameter reported by Langer *et al.*[52] of 5.6 meV. The latter was in good agreement with the theoretical calculation by Rohner,[53] which only includes the short-range contribution. The value in Langer *et al.*[52] is obtained from a uniaxial stress measurement which strictly speaking measures a combination of a stress deformation potential and the exchange parameter. Skettrup and Balslev[39] provide an alternative analysis of the date of Langer *et al.*[52]

Having identified the main Γ_5 peak in the data of Reynolds *et al.* as the Γ_{5L}, the question then comes up as to why Reynolds *et al.*[8] in $\mathbf{E}\perp\mathbf{c}$ see the Γ_5 state at almost exactly the same energy as the longitudinal exciton instead of at the tranverse Γ_{5T}. This is most likely explained by the polariton effect.[47] The reason why primarily the upper branch of the polariton is visible in the experiment of Reynolds *et al.* is not clear but such an interpretation would seem to be consistent with the results of Blattner *et al.*[47] on polariton dispersion calculations. The behavior for $\mathbf{E}\perp\mathbf{c}$ and $\mathbf{H}\|\mathbf{c}$ is further discussed in Hümmer *et al.*[51] and involves coupling with the linear in $\mathbf{k}$ terms. Since these are absent for Γ_9, it is, according to those authors, further evidence of the Γ_7 symmetry of the VBM.

VI. CONCLUSION

The main conclusion of this paper is that the original Thomas assignment of the valence band maximum as having Γ_7 symmetry is confirmed by (1) a direct first-principles band structure calculation and (2) a careful analysis of the recent magneto-optical data on excitons by Reynolds *et al.*[8] includ-

ing exciton coupling and a calculation of the hole g factors within the Luttinger model.

The origin of the anomalous ordering is the effective negative spin-orbit coupling which arises from the contribution of the-lower lying Zn $3d$ bands. The conclusion of a negative spin-orbit coupling is found to be robust when effects beyond the the LDA on the Zn $3d$-band position are included and an optimal value value for the latter was derived which gives good agreement with the basic valence-band splittings. The effective mass parameters of the valence and conduction bands are obtained from these band structure calculations and used in the exciton model.

The exciton calculations show that the coupling of the excitons leads to only small differences in the exciton binding energies derived from the three valence-band maxima. The differences in binding energy are smaller than the splittings of the valence bands themselves. Thus, the primary character of the lowest-level exciton is clearly that corresponding to the top valence band.

The calculations of the magnetic-field-induced splittings of the excitons show that our model is consistent with the experimental data. The discrepancy with the interpretation of Reynolds *et al.*[8] is that they assumed a positive hole g factor, whereas our calculations indicate that the hole g factor for the the Γ_7 valence band is in fact negative. Furthermore, the effective g for the hole in an exciton is shown to strongly depend on the exciton state.

ACKNOWLEDGMENTS

The work at CWRU was supported by the ONR under Grant No. N000-99-1-1073 and N000-14-98-1-0160. A.V.R. gratefully acknowledges financial support from the Alexander von Humboldt Foundation. We thank A. Hoffmann for bringing Ref. 48 to our attention.

*On leave from A. F. Ioffe Physico-technical Institute, 194021, St.-Petersburg, Russia.

[1] D.G. Thomas, J. Phys. Chem. **15**, 86 (1960).

[2] We here follow the notation of Bir and Pikus (Ref. 3) for the symmetry labeling of the irreducible representations of the wurtzite group C_{6v} in which the valence-band maximum has Γ_5 symmetry. Note that in many recent papers a different notation is followed, one in which Γ_6 and Γ_5 are interchanged.

[3] G. L. Bir and G. E. Pikus, *Symmetry and Strain-Induced Effects in Semiconductors* (Wiley, New York, 1974).

[4] W.Y. Liang and A.D. Yoffe, Phys. Rev. Lett. **20**, 59 (1968).

[5] Y.S. Park, C.W. Litton, T.C. Collins, and D.C. Reynolds, Phys. Rev. **143**, 512 (1966).

[6] D.C. Reynolds, C.W. Litton, and T.C. Collins, Phys. Rev. A **140**, A1726 (1965).

[7] B. Segall, Phys. Rev. **163**, 769 (1967).

[8] D.C. Reynolds, D.C. Look, B. Jogai, C.W. Litton, G. Cantwell, and W.C. Harsch, Phys. Rev. B **60**, 2340 (1999).

[9] M. Cardona, Phys. Rev. **129**, 69 (1963).

[10] K. Shindo, A. Morita, and H. Kamimura, J. Phys. Soc. Jpn. **20**, 2054 (1965).

[11] R.T. Girard, O. Tjernberg, G. Chiaia, S. Söderholm, U.O. Karsson, C. Wigren, H. Nylén, and I. Lindau, Surf. Sci. **373**, 409 (1997).

[12] W.R.L. Lambrecht, K. Kim, S.N. Rashkeev, and B. Segall, in *Gallium Nitride and Related Materials*, edited by R.D. Dupuis, F.A. Ponce, S. Nakamura, and J.A. Edmond, Mater. Res. Soc. Symp. Proc. No. 395 (Materials Research Society, Pittsburgh, 1996), p. 455.

[13] O.K. Andersen, Phys. Rev. B **12**, 3060 (1975); O. K. Andersen, O. Jepsen, and M Šob, in *Electronic Band Structure and its Applications*, edited by M. Yussouf (Springer, Heidelberg, 1987), p. 1.

[14] M. Methfessel, Phys. Rev. B **38**, 1537 (1988).

[15] P. Hohenberg and W. Kohn, Phys. Rev. B **136**, B864 (1964).

[16] A.V. Rodina, M. Dietrich, A. Göldner, L. Eckey, A. Hoffmann, Al. L. Efros, M. Rosen, and B.K. Meyer, Phys. Rev. B **64**, 115204 (2001).

[17] J.M. Luttinger, Phys. Rev. **102**, 1030 (1956); J.M. Luttinger and W. Kohn, *ibid.* **97**, 869 (1955).

[18] G. Dresselhaus, A.F. Kip, and C. Kittel, Phys. Rev. **98**, 368 (1955).

[19] L. Hedin and B.I. Lundqvist, J. Phys. C **4**, 2064 (1971).

[20] K. Kim, W.R.L. Lambrecht, and B. Segall, Phys. Rev. B **53**, 16 310 (1996); and **56**, 7018 (1997).

[21] P. Schröer, P. Krüger, and J. Pollmann, Phys. Rev. B **47**, 6971 (1993).

[22] Y.-N. Xu and W.Y. Ching, Phys. Rev. B **48**, 4335 (1993).

[23] "G" stands for the one-particle Greens' function and "W" for the screened Coulomb interaction in the first approximation to the self-energy operator in the so-called GW theory of Hedin and Lundqvist (Ref. 24).

[24] L. Hedin and S. Lundqvist, Solid State Phys. **23**, 1 (1969).

[25] D. Vogel, P. Krüger, and J. Pollmann, Phys. Rev. B **52**, R14316 (1995).

[26] K. Kim, W.R.L. Lambrecht, B. Segall, and M. van Schilfgaarde, Phys. Rev. B **56**, 7363 (1997).

[27] F. Herman and S. Skillman, *Atomic Structure Calculations* (Prentice-Hall, Englewood Cliffs, NJ, 1963).

[28] K. Hümmer, Phys. Status Solidi B **56**, 249 (1973).

[29] M. Cardona, J. Phys. Chem. Solids **24**, 1543 (1963).

[30] W.S. Baer, Phys. Rev. **154**, 785 (1967).

[31] K.J. Button, D.R. Cohm, M. von Ortenverger, B. Lax, E. Mollwo, and R. Helbig, Phys. Rev. Lett. **28**, 1637 (1972).

[32] A. Baldereschi and N.C. Lipari, Phys. Rev. B **3**, 439 (1971).

[33] M. Altarelli and N.C. Lipari, Phys. Rev. B **7**, 3798 (1973).

[34] J. Pollmann and H. Büttner, Phys. Rev. B **16**, 4480 (1977).

[35] T.V. Butkhuzi, T.G. Chelidze, A.N. Georgobiani, D.L. Jashiashvili, T.G. Khulordava, and B.E. Tsekvava, Phys. Rev. B **58**, 10 692 (1998).

[36] H. Yoshikawa and S. Adacchi, Jpn. J. Appl. Phys., Part 1 **36**, 6237 (1997).

[37] R.J. Elliott, Phys. Rev. **124**, 340 (1961).

[38] R. S. Knox, Theory of Excitons, in *Solid State Physics, Advances in Research and Applications*, edited by F. Seitz and D. Turnbull (Academic Press, New York 1963), Suppl. 5.

[39] T. Skettrup and I. Balslev, Phys. Status Solidi **40**, 93 (1970).

[40] M.M. Denisov and V.P. Makarov, Phys. Status Solidi B **56**, 9 (1973).

[41] J. Flohrer, E. Jahne, and M. Porsch, Phys. Status Solidi B **91**, 467 (1979).
[42] K. Cho, Phys. Rev. B **14**, 4463 (1976).
[43] D. Block, A. Herve, and R.T. Cox, Phys. Rev. B **25**, 6049 (1982).
[44] D. M. Hofmann, A. Hofstaetter, F. Leiter, H. Zhou, F. Henecker, B. K. Meyer, S. B. Orlinskii, J. Schmidt, and P. G. Baranov, Phys. Rev. Lett. **88**, 045504 (2002).
[45] P.A. Shields, R.J. Nicholas, F.M. Peeters, B. Beaumont, and P. Gibart, Phys. Rev. B **64**, 081203(R) (2001).
[46] J. Campo, M. Julier, D. Coquillat, J.P. Lascaray, D. Scalbert, and O. Briot, Phys. Rev. B **56**, R7108 (1997).
[47] G. Blattner, G. Kurtze, G. Schmieder, and C. Klingshirn, Phys. Rev. B **25**, 7413 (1982),
[48] M. Rosenzweig, Diploma thesis, Technical Univiversity of Berlin, 1976.
[49] J.J. Hopfield and D.G. Thomas, J. Phys. Chem. Solids **12**, 276 (1960).
[50] R. Kuhnert, R. Helbig, and K. Hümmer, Phys. Status Solidi B **107**, 83 (1981).
[51] K. Hümmer, R. Helbig, and M. Baumgärtner, Phys. Status Solidi B **86**, 527 (1978).
[52] D.W. Langer, R.N. Euwema, K. Era, and T. Koda, Phys. Rev. B **2**, 4005 (1970).
[53] P.G. Rohner, Phys. Rev. B **3**, 433 (1971).